$NaSc(BH_4)_4$: A Novel Scandium-Based Borohydride

Radovan Černý,*,† Godwin Severa,‡ Dorthe B. Ravnsbæk,§ Yaroslav Filinchuk,|| Vincenza D'Anna,⊥ Hans Hagemann,⊥ Dörthe Haase,# Craig M. Jensen,*,‡ and Torben R. Jensen*,§

Laboratory of Crystallography, University of Geneva, 1211 Geneva, Switzerland, Department of Chemistry, University of Hawaii at Manoa, 2545 The Mall, Honolulu, Hawaii 96822-227, Interdisciplinary Nanoscience Center (iNANO) and Department of Chemistry, University of Aarhus, Langelandsgade 140, DK-8000 Århus C, Denmark, Swiss-Norwegian Beamlines at ESRF, BP-220, 38043 Grenoble, France, Department of Physical Chemistry, University of Geneva, 1211 Geneva, Switzerland, and MAX-lab, Lund University, S-22100 Lund, Sweden

Received: August 31, 2009; Revised Manuscript Received: November 19, 2009

A new alkaline transition-metal borohydride, $NaSc(BH_4)_4$, is presented. The compound has been studied using a combination of in situ synchrotron radiation powder X-ray diffraction, thermal analysis, and vibrational and NMR spectroscopy. $NaSc(BH_4)_4$ forms at ambient conditions in ball-milled mixtures of sodium borohydride and $ScCl_3$. A new ternary chloride Na_3ScCl_6 ($P2_1/n$, $a = 6.7375(3)$ Å, $b = 7.1567(3)$ Å, $c = 9.9316(5)$ Å, $\beta = 90.491(3)°$, $V = 478.87(4)$ Å^3), isostructural to Na_3TiCl_6, was identified as an additional phase in all samples. This indicates that the formation of $NaSc(BH_4)_4$ differs from a simple metathesis reaction, and the highest scandium borohydride yield (22 wt %) was obtained with a reactant ratio of $ScCl_3/NaBH_4$ of 1:2. $NaSc(BH_4)_4$ crystallizes in the orthorhombic crystal system with the space group symmetry *Cmcm* ($a = 8.170(2)$ Å, $b = 11.875(3)$ Å, $c = 9.018(2)$ Å, $V = 874.9(3)$ Å^3). The structure of $NaSc(BH_4)_4$ consists of isolated homoleptic scandium tetraborohydride anions, $[Sc(BH_4)_4]^-$, located inside slightly distorted trigonal Na_6 prisms (each second prism is empty, triangular angles of 55.5 and 69.1°). The experimental results show that each Sc^{3+} is tetrahedrally surrounded by four BH_4 tetrahedra with a 12-fold coordination of H to Sc, while Na^+ is surrounded by six BH_4 tetrahedra in a quite regular octahedral coordination with a (6 + 12)-fold coordination of H to Na. The packing of Na^+ cations and $[Sc(BH_4)_4]^-$ anions in $NaSc(BH_4)_4$ is a deformation variant of the hexagonal NiAs structure type. $NaSc(BH_4)_4$ is stable from RT up to ~410 K, where the compound melts and then releases hydrogen in two rapidly occurring steps between 440 and 490 K and 495 and 540 K. Thermal expansion of $NaSc(BH_4)_4$ between RT and 408 K is anisotropic, and lattice parameter *b* shows strong anomaly close to the melting temperature.

Introduction

Metal borohydrides are of interest for hydrogen storage in mobile applications.[1,2] Borohydrides of alkaline and alkaline earth metals desorb a large quantity of hydrogen (up to 20.8% for $Be(BH_4)_2$), although the decomposition temperatures are usually high.[3] On the other hand, most known borohydrides of transition metals, especially of 3d metals, are unstable.[3] The decomposition temperatures of single-cation borohydrides were recently empirically related (through the enthalpy of formation) to the Pauling electronegativity of the cation.[4] Preparation of bimetallic (alkaline or alkaline earth and transition-metal) borohydrides appears to be a promising new route for tuning the thermodynamic properties of borohydride-based hydrogen storage materials.[5] This approach suggests using heavier transition-metal ions with higher electronegativities, which unfortunately will decrease the gravimetric capacities.

Metal borohydrides are known to form a variety of structure types. Compounds such as $Al(BH_4)_3$, $Zr(BH_4)_4$, and $Hf(BH_4)_4$ form molecular compounds, whereas, for example, $Ca(BH_4)_2$ and $Mg(BH_4)_2$ form three-dimensional network structures.[6] Furthermore, the recent study of alkali zinc borohydrides shows a variety of compositions and structural topologies. The compounds $LiZn_2(BH_4)_5$ and $NaZn_2(BH_4)_5$ are built of two identical interpenetrated three-dimensional frameworks consisting of isolated complex anions, $[Zn_2(BH_4)_5]^-$, whereas $NaZn(BH_4)_3$ consists of a single three-dimensional network, containing polymeric anions with the composition $[Zn(BH_4)_3]_n^{n-}$.[7] Bimetallic heteroleptic borohydrides are also known, for example, $KZn(BH_4)Cl_2$, that contain the composite anion $[Zn(BH_4)Cl_2]^-$.[8] Thus, structural studies of novel bimetallic borohydrides might hold the key to gain further insight of trends within the thermal stability of bimetallic borohydrides.

We have recently characterized the crystal structure of the first alkaline transition-metal bimetallic homoleptic borohydride, $LiSc(BH_4)_4$, prepared by mechanochemical synthesis.[9] The desorption properties of the same compound were studied recently, showing the release of about 6.4 wt % of the initial hydrogen content at 673 K.[10] This reaction, however, did not show a complete reversibility. Here, we report on the crystal

* To whom correspondence should be addressed. E-mail: Radovan.Cerny@unige.ch (R.C.), jensen@hawaii.edu (C.M.J.), trj@chem.au.dk (T.R.J.). Tel: +41 22 379 6450 (R.C.), +1 808 956 2769 (C.M.J.), +45 8942 3894 (T.R.J.). Fax: +41 22 379 6108 (R.C.), +1 808 956 5908 (C.M.J.), +45 8619 6199 (T.R.J.).

† Laboratory of Crystallography, University of Geneva.

‡ University of Hawaii at Manoa.

§ University of Aarhus.

|| Swiss-Norwegian Beamlines at ESRF.

⊥ Department of Physical Chemistry, University of Geneva.

Lund University.

10.1021/jp908397w
Published on Web 12/23/2009

structure; desorption properties; and Raman, infrared, and NMR spectra of another scandium-based bimetallic borohydride, $NaSc(BH_4)_4$.

Experimental Section

Synthesis. The preparation and manipulation of all samples were performed in an argon-filled glovebox with a circulation purifier ($p(O_2, H_2O) < 0.1$ ppm).

For samples **A** (prepared in Hawaii), anhydrous scandium chloride, $ScCl_3$ (Alfa Aesar, 99.9%), and sodium borohydride, $NaBH_4$ (Sigma-Aldrich, 98%), were combined in the molar ratios of 1:2 and 1:4 and ball-milled under inert conditions (argon atmosphere) in a Fritsch Pulverisette planetary mill using 65 mL stainless steel containers using an approximately 1:35 ratio of sample to 10 mm balls. The 1:2 and 1:4 samples were milled at 350 rpm for 20 and 60 h, respectively.

For samples **B** (prepared in Aarhus), anhydrous scandium chloride, $ScCl_3$ (Sigma-Aldrich, 99.7%), and sodium borohydride, $NaBH_4$ (Sigma-Aldrich, 98.5%), were combined in the molar ratios of 1:2, 1:3, and 1:4 and ball-milled for 120 min under inert conditions (argon atmosphere) in a Fritsch Pulverisette planetary mill using 80 mL tungsten carbide steel containers using an approximately 1:35 ratio of sample to 10 mm balls.

A sample of $LiSc(BH_4)_4$ was prepared in Aarhus by ball-milling a mixture of $LiBH_4$ (98.5%, Sigma-Aldrich) and $ScCl_3$ (Sigma-Aldrich, 99.7%) in the molar ratio of 4:1, as described previously.[9] This sample is used for the comparison with the new compound presented in this study.

Laboratory X-ray Powder Diffraction (PXD). All samples **B** were initially investigated using in-house powder X-ray diffraction (PXD) in order to identify the reaction products and estimate the crystallinity of the samples. PXD measurements were performed in Debye−Scherrer transmission geometry using a Stoe diffractometer equipped with a curved Ge(111) monochromator (Cu $K\alpha_1$ radiation, $\lambda = 1.54060$ Å) and a curved position sensitive detector. Data were collected at room temperature (RT) between 4 and 127° 2θ with a counting time of ~960 s per step. All samples were mounted in a glovebox in 0.4 mm glass capillaries sealed with glue.

Thermal Analysis. Simultaneous thermogravimetric analysis (TG) and differential scanning calorimetry (DSC) were performed using a Netzsch STA449C Jupiter instrument (heating rate = 2 K/min, RT to 773 K) and corundum crucibles with lids as sample holder. The experiments were conducted in a helium (4.6) atmosphere using samples **B** and $LiSc(BH_4)_4$.

Thermal desorption of sample **A** 2:1 was performed in an initially evacuated stainless steel reactor using a Suzuki Shokan PCT-2SDWIN Sievert type apparatus, by ramping the temperature from room temperature to 673 K with a 1.5 h hold at maximum temperature. The temperature fluctuation at the maximum was on average about ± 5 K.

In Situ Time-Resolved Synchrotron Powder Diffraction (SR-PXD). One set of SR-PXD was collected on samples **A** at the Swiss-Norwegian Beamlines (SNBL) at the European Synchrotron Radiation Facility (ESRF) in Grenoble, France. A glass capillary (o.d. = 1 mm) with the sample was heated from RT to 500 K at a rate of 1 K/min while synchrotron powder diffraction data (PXD) were collected. The temperature was controlled with the Oxford Cryostream 700+. The data were collected using a MAR345 image plate detector at a sample-to-detector distance of 400 mm and radiation with selected wavelengths of $\lambda = 0.66863$ or 0.769748 Å. The capillary was oscillated by 60° during exposure to the X-ray beam for 60 s, followed by a readout for ~83 s.

Another set of SR-PXD data was collected on samples **B** at the beamline I911-5 of the synchrotron MAXII, Lund, Sweden, in the research laboratory MAX-Lab with a MAR165 CCD detector system and selected wavelength of 0.9077 Å.[11] The CCD camera exposure time was 30 s. The sample cell was specially developed for studies of gas/solid reactions and allows high pressure and temperature to be applied.[12,13] The powdered samples were mounted in a sapphire single-crystal tube (o.d., 1.09 mm; i.d., 0.79 mm) in an argon-filled glovebox ($p(O_2, H_2O) < 1$ ppm). The sample holder was sealed inside the glovebox. The temperature was controlled with a thermocouple placed in the sapphire tube 1 mm from the sample. The samples were typically heated from RT to 773 K with a heating rate of 5 K/min.

All obtained raw images were transformed to 2D-powder diffraction patterns using the FIT2D program,[14] which was also used to remove diffraction spots from the single-crystal sapphire tube used as sample holder.

Structure Solution. The SR-PXD data measured for the 2:1 mixtures (**A** and **B**) showed the presence of Na_3ScCl_6 as a major phase in the sample, that is, corresponding to ~78 wt % and ~58 mol %. The remaining fraction of the samples is mainly $NaSc(BH_4)_4$, that is, ~22 wt % and ~42 mol %. The nine observed peaks of $NaSc(BH_4)_4$, identified as diffraction peaks from sample **A** that simultaneously vanish at 410 K, were indexed with DICVOL04[15] in the orthorhombic lattice with $a = 8.170(2)$ Å, $b = 11.875(3)$ Å, $c = 9.018(2)$ Å, and $V = 874.9(3)$ Å^3 at RT. Initially, systematic extinctions were not easily recognized, leading to several possible space groups. In the next iteration, space group $C222_1$ was selected and the structure was solved with the direct space method program FOX[16] and refined with the Rietveld method using the TOPAS program.[17] Finally, with the help of a symmetry checking routine ADDSYM in the program PLATON,[18] the correct space group *Cmcm* was identified. The resulting structure containing one Na atom (position 4*a*), one Sc atom (position 4*c*), and two BH_4 groups (two positions of the boron atom 8*f* and 8*g*) in the asymmetric unit was refined by the Rietveld method. The structure was solved and refined with the BH_4 groups as semirigid ideal tetrahedra with one common refined B−H distance. As both boron atoms are situated on the mirror plane symmetry, both BH_4 tetrahedra were allowed only to translate and to rotate following the mirror plane symmetry. No antibump distance restraints were used. The displacement parameters were refined isotropically with three independent parameters (one for each atom type), however, that of boron refined to the lower limit of 1 and that of hydrogen to the upper limit of 4. The uncertainties of crystallographic coordinates of hydrogen atoms were not available from the least-squares matrix and were estimated by the bootstrap method.[19] The agreement factors are R_{wp} (not corrected for background) = 1.56%, R_{wp} (corrected for background) = 3.57%, $\chi^2 = 27$, R_{Bragg} ($NaSc(BH_4)_4$) = 0.60%, and R_{Bragg} (Na_3ScCl_6) = 0.93%. The high value of χ^2 reflects mainly the extremely high counting statistics of the powder diffraction data obtained from modern 2D-detectors. The refined atomic positions of $NaSc(BH_4)_4$ are found in the Supporting Information in Table S1, selected bond distances and angles on the $[Sc(BH_4)_4]^-$ anion in Table S2, and the Rietveld plot is shown in Figure S1. The refined atomic positions of Na_3ScCl_6 are found in Table S3 (Supporting Information).

Raman and Infrared (IR) Spectroscopy. Raman spectra were obtained on sample **A** 2:1 using a Kaiser Holospec monochromator in conjunction with a liquid-nitrogen-cooled CCD camera. Spectra were excited using the laser wavelength

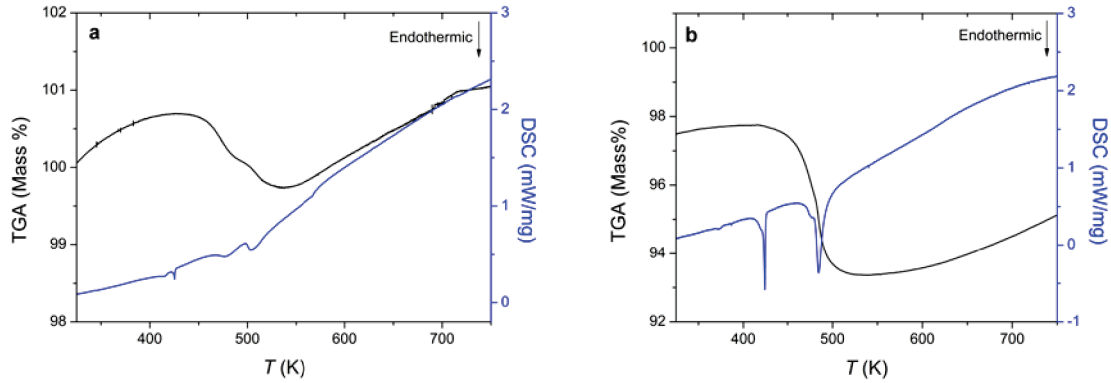

Figure 1. TGA−DSC data for a sample containing (a) $NaSc(BH_4)_4$ and Na_3ScCl6 (sample **B**) and (b) $LiSc(BH_4)_4$ and LiCl.

of 488 nm with a typical laser power of 50 mW. The spectral resolution of the Raman spectra is about 3 cm^{-1}. The samples were sealed in melting point capillaries.

IR spectra were measured on sample **A** 2:1 using a Biorad Excalibur instrument equipped with a Specac low-temperature Golden Gate diamond ATR system. The spectral resolution was set to 1 or 2 cm^{-1} for the different experiments. Samples were loaded in the glovebox in the ATR system.

NMR Spectroscopy. Solid-state NMR spectra were collected on sample **A** 2:1 using a Varian Inova spectrometer equipped with a 3.2 mm HX cross-polarization magic-angle spinning (CPMAS) probe (Varian Chemagnetics, Ft. Collins, CO) at 128.3, 97.2, and 105.8 MHz for ^{11}B, ^{45}Sc, and ^{23}Na nuclei, respectively. The sample was packed into 3.2 mm rotors and spun at rates of 10−12 kHz. Single-pulse excitation with pulse widths of 1.0, 0.8, and 6.0 μs were used for ^{11}B, ^{23}Na, and ^{45}Sc nuclei, respectively. The acquisition times were between 10 and 20 ms. CPMAS were obtained in sudden passage regime using weak RF fields (V_{1H} < 25 kHz, V_{1Sc} < 60 kHz, and V_{1Na} < 25 kHz) and cross-polarization mixing times of 500 μs. Frequencies are reported with respect to the following standards set to 0 ppm: boron trifluoride etherate for ^{11}B NMR, aqueous $ScCl_3$ for ^{45}Sc, and saturated aqueous NaCl solution for ^{23}Na NMR.

Results and Discussion

Synthesis and Initial Phase Analysis. For the system $LiBH_4$−$ScCl_3$, only one metathesis reaction occurs during ball-milling, which produces the products $LiSc(BH_4)_4$ and LiCl. In contrast, the $NaBH_4$−$ScCl_3$ samples contain two sets of unidentified Bragg peaks. One of these new sets of Bragg peaks was assigned to $NaSc(BH_4)_4$ and the other was assigned to a new ternary sodium scandium chloride Na_3ScCl_6, which is isostructural to Na_3TiCl_6[20] and was identified as an additional phase in all samples. Furthermore, the samples with the starting ratios of $NaBH_4/ScCl_3$ of 3:1 and 4:1 contain $NaBH_4$ in different amounts, according to the starting ratio, whereas no diffraction can be assigned to $ScCl_3$. The samples with the starting ratio of 2:1 show neither $ScCl_3$ nor $NaBH_4$ peaks and appear to contain the largest fraction of the new compound, $NaSc(BH_4)_4$. The PXD data show no presence of NaCl in any sample, which indicates that the reaction during the ball-milling differs from the simple metathesis reaction, which has previously been suggested,[21] and can be described as

$$4NaBH_4 + 2ScCl_3 \rightarrow NaSc(BH_4)_4 + Na_3ScCl_6 \quad (1)$$

indicating that the optimal starting ratio between $NaBH_4$ and $ScCl_3$ is 2:1. Reaction 1 may consist of two subreactions, that is, possibly formation of NaCl as an intermediate via a metathesis reaction, followed by fast formation of Na_3ScCl_6 via an addition reaction. Due to the formation of the ternary chloride Na_3ScCl_6, the maximal borohydride yield is 22 wt %.

Thermal Analysis. The results from TGA and DSC analysis displayed in Figure 1a are for sample **B** 2:1. Thermal events observed by DSC are listed in the Supporting Information in Table S4. The slope observed in the DSC data and the continuous small increase in the TGA data are instrumental artifacts due to buoyancy. In all cases, alkali halide salts, NaCl or LiCl, were identified by PXD in the residue after the thermal analysis experiments. The results of TGA−DSC for sample $LiBH_4$−$ScCl_3$ in the ratio of 4:1 are shown for comparison in Figure 1b.

The mass loss in the $NaSc(BH_4)_4$ sample (see Figure 1a) appears to occur in two rapid steps between approximately 440 and 490 K and 495 and 540 K. Small endothermic peaks are observed in the DSC data at ∼425, 478, and ∼504 K. The first peak is sharp and may correspond to melting of one of the reaction products. The latter two thermal events seem to proceed over wide temperature intervals of 462−896 K and 498−565 K, respectively. These temperature intervals correspond with the two observed ranges for the mass loss. Observation of two decomposition steps indicates the complexity of the decomposition, suggesting that $NaSc(BH_4)_4$ and Na_3ScCl_6 react during heating; for example, $NaBH_4$ might form as an intermediate decomposition product from $NaSc(BH_4)_4$ and react with Na_3ScCl_6 upon further heating, possibly during formation of an amorphous ScB_x phase. Both of these processes would likely result in the release of hydrogen.

The observed total mass loss is 0.97 wt %, whereas the calculated hydrogen content in the sample is 3.56 wt %. The discrepancy between the observed and calculated mass loss might be due to a short exposure to air of the sample during its transfer to the TGA−DSC instrument. The thermal desorption profile of sample **A** 2:1 (Figure 2) shows 3.04 wt % of desorbed hydrogen, close to the calculated hydrogen content. This suggests that the mass loss corresponds to the release of hydrogen gas only (no diborane); hence, boron remains in the solid dehydrogenated sample, which is the first requisite for reversible hydrogen storage.

Mass loss in the $LiSc(BH_4)_4$ sample (see Figure 1b) occurs in the temperature range of 415−535 K. Endothermic events are observed with peak values at ∼424, ∼476, and ∼484 K, corresponding to the temperature interval for the observed mass loss. The observation of several endothermic events during decomposition suggests that it involves several processes. The observed total mass loss is 4.38 wt %, whereas the calculated hydrogen content in the sample is 6.76 wt %. The thermal events

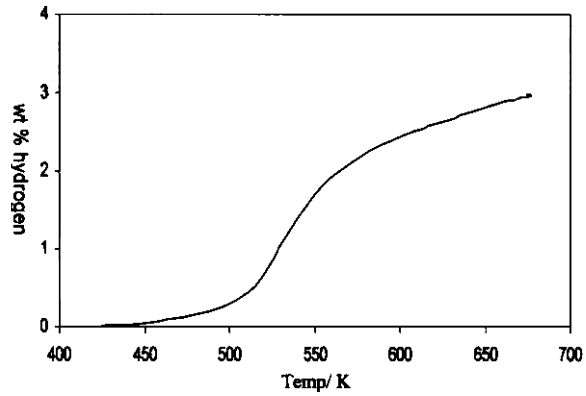

Figure 2. Thermal desorption profile of ball-milled $2NaBH_4 + ScCl_3$ (sample **A**). Maximum desorbed hydrogen is 3.04 wt %.

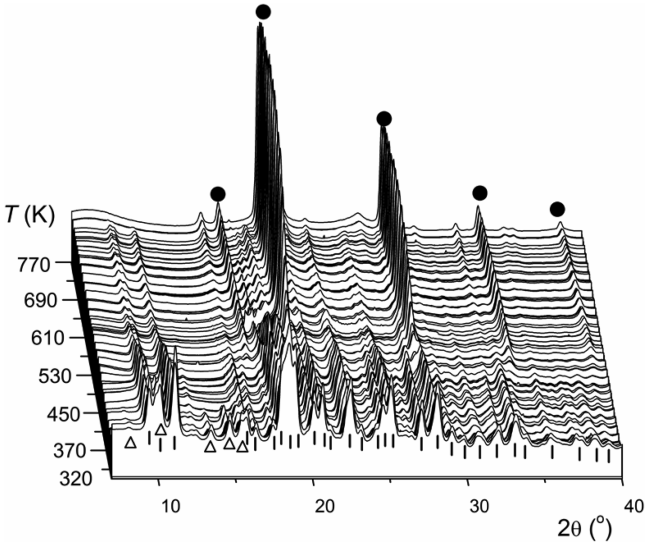

Figure 3. In situ synchrotron radiation powder X-ray diffraction measured for the ball-milled $2NaBH_4 + ScCl_3$ (sample **B**) heated from RT to 773 K with a heating rate of 5 K/min and $p(H_2) \sim 2.5$ bar ($\lambda = 0.9077$ Å). Only peaks that are at least partly resolved are marked by the symbols: Δ $NaSc(BH_4)_4$, |Na_3ScCl_6 and ● NaCl.

observed for $LiSc(BH_4)_4$ are sharp as compared with those for $NaSc(BH_4)_4$, which may reflect differences in the desorption kinetics.

In Situ SR-PXD. Figure 3 shows in situ SR-PXD data for sample **B** 2:1. At RT, $NaSc(BH_4)_4$ and Na_3ScCl_6 are present. The peaks corresponding to $NaSc(BH_4)_4$ disappear at ~410 K, likely due to melting since only an endothermic peak and no mass loss were observed in this temperature region by thermal analysis. The diffraction from Na_3ScCl_6 decreases between 430 and 540 K. In this temperature range, NaCl is formed by a reaction between Na_3ScCl_6 and the melt of $NaSc(BH_4)_4$. The reaction will lead to the release of hydrogen, according to TGA in which a mass loss was observed in this temperature range. Upon further increase of the temperature, an unidentified compound forms at ~690 K, and its content is still increasing up to 773 K. This is possibly a scandium boride, that is, ScB_x, formed as a decomposition product. As the temperature increases, this compound crystallizes. The samples of higher molar ratios, that is, 3:1 and 4:1, were also investigated using in situ SR-PXD. The data for these samples show a presence of $NaBH_4$ at RT. As diffraction from Na_3ScCl_6 decreases, diffraction peaks from $NaBH_4$ slowly change 2θ position and continuously approach the positions of the NaCl peaks. This suggests that Na_3ScCl_6 reacts with $NaBH_4$ and that a solid solution $Na(BH_4)_{1-x}Cl_x$ is formed during ball-milling, as was recently found for $LiBH_4 + LiCl$ mixtures.[22,23]

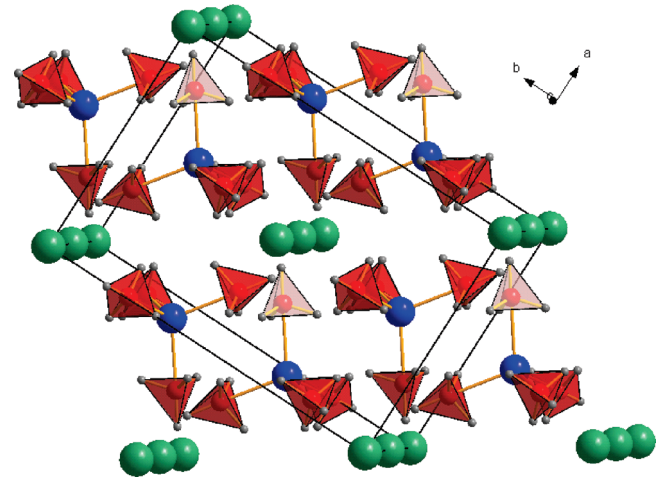

Figure 4. Crystal structure of $NaSc(BH_4)_4$ viewed approximately along the *c* axis, showing the coordination of Sc atoms (blue) by BH_4 tetrahedra (red); Na atoms are in green.

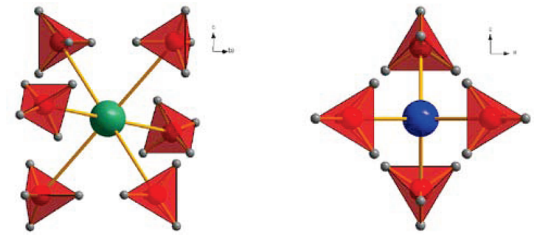

Figure 5. Coordination of Na atoms (green) and Sc atoms (blue) by BH_4 tetrahedra (red).

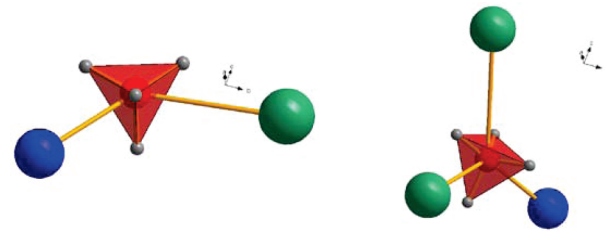

Figure 6. Coordination of B1 (left) and B2 (right) atoms (red) by Sc atoms (blue) and Na atoms (green).

Crystal Structure. The structural drawing of $NaSc(BH_4)_4$ viewed approximately along the *c* axis is given in Figure 4. The basic structural building unit of $NaSc(BH_4)_4$ is the borohydride complex BH_4^-, which is a regular tetrahedron. A single B−H distance of 1.13(2) Å was refined for the rigid BH_4 tetrahedra. It compares well with those refined with single-crystal X-ray diffraction data in related borohydrides, such as $Mg(BH_4)_2$ (1.08−1.22 Å[24]) and $NaBH_4$ and its dihydrate, $NaBH_4 \cdot 2H_2O$ (1.09−1.13 Å[25]).

The scandium atom is surrounded by four BH_4 tetrahedra (see Figure 5), forming a nearly regular tetrahedral environment (distances Sc−B within 2.27(1)−2.50(1) Å, angles B−Sc−B within 108.9(5)−110.6(6)°). This coordination resembles (Table S2, Supporting Information) the almost ideal tetrahedral $[Sc(BH_4)_4]^-$ anion, as found by DFT optimization of the isolated $[Sc(BH_4)_4]^-$ anion[9] and is less deformed than the experimentally observed $[Sc(BH_4)_4]^-$ anion in $LiSc(BH_4)_4$.[9] The tetrahedral coordination of transition-metal cations by four BH_4^- anions is common also for cations in many other metal borohydrides:[6] Mg^{2+} in $Mg(BH_4)_2$,[24,26] Li^+ in three of the four known phases

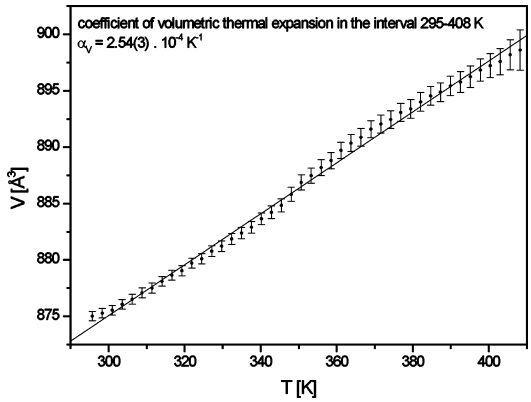

Figure 7. Cell volume of $NaSc(BH_4)_4$ as a function of temperature.

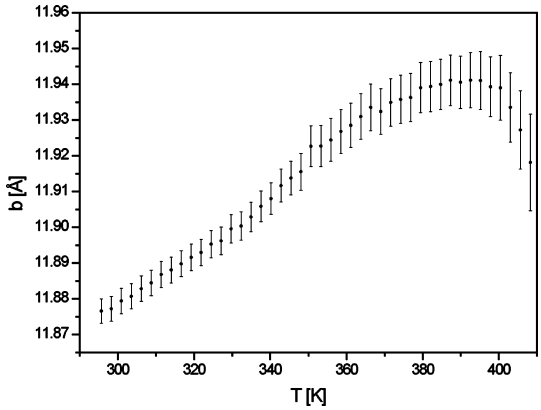

Figure 8. Lattice parameter *b* of $NaSc(BH_4)_4$ as a function of temperature.

of $LiBH_4$[27−29] and in $LiK(BH_4)_2$,[30] for Zr^{4+} in $Zr(BH_4)_4$ at 113 K,[31] and for Sc^{3+} in $LiSc(BH_4)_4$.[9]

On the other hand, the sodium atom is surrounded by six BH_4 tetrahedra (see Figure 5) in a quite regular octahedral coordination with Na−B distances within 2.94(1)−3.22(1) Å, B−Na−B angles in the range of 87.76(2)−92.24(2)°, which is close to the values for an ideal octahedron, as observed in the cubic $NaBH_4$[25] at ambient conditions, and to the slightly deformed octahedron in the tetragonal low-temperature and orthorhombic high-pressure $NaBH_4$.[32]

The structure of $NaSc(BH_4)_4$ is found to contain two independent BH_4^- anions with different coordinations (see Figure 6). One borohydride, B1, is coordinated by one scandium and one sodium atom with a Sc−B−Na angle of 132.3(5)°, which is common in metal borohydrides.[6] The other borohydride, B2, found in the asymmetric unit, coordinates to one scandium and two sodium atoms, forming a nearly flat triangular coordination; that is, the distance from B2 to the Na−Sc−Na plane is 0.49(1) Å and the angles in the Na−Sc−Na triangle range from 53.86(1) to 63.07(2)°, as it was observed only in β-$Ca(BH_4)_2$[33,34] and in the recently characterized $NaZn(BH_4)_3$.[7]

The mode of BH_4^- coordination by scandium and sodium atoms is determined only approximately using the structural model with pseudorigid ideal BH_4^- tetrahedra. It is, however, important to notice that no antibump restraints were needed to stabilize the Rietveld refinement, unlike for the similar compound $Mn(BH_4)_2$.[35] The coordination mode for the BH_4^- anion to scandium corresponds to the cation···H_3B scheme; that is, the BH_4^- anion has a plane of three H atoms oriented toward the cation. It results in a 12-fold coordination of Sc to hydrogen with Sc−H distances in the range of 2.15(2)−2.17(2) Å. Sodium has (6 + 12)-fold coordination to hydrogen with 6 short Na−H distances of 2.33(1)−2.63(1) Å and 12 longer distances of 3.01(1)−3.34(1) Å. The coordination of Na differs from the 12-fold, as found in all three known phases of $NaBH_4$[25,32] with a Na−H distance of 2.58 Å in the cubic $NaBH_4$ at ambient conditions and of 2.44−2.59 Å in the tetragonal $NaBH_4$ at 10 K.

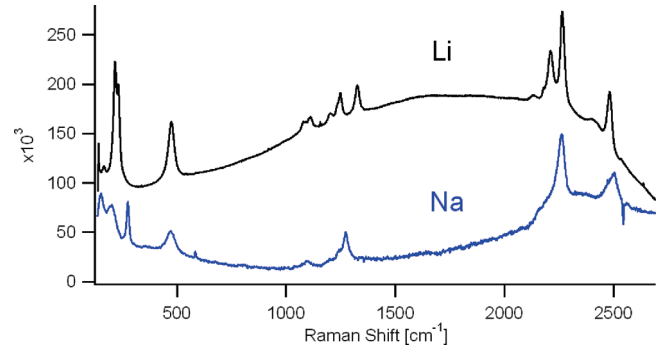

Figure 9. Raman spectra of alkali metal−scandium borohydrides.

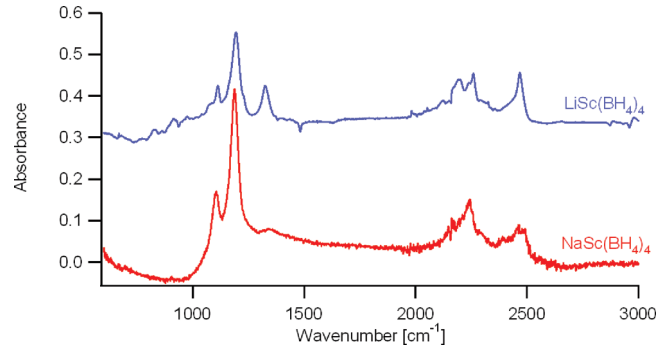

Figure 10. Infrared spectra of $NaSc(BH_4)_4$ (300 K) and $LiSc(BH_4)_4$ (∼220 K). The jump appearing around 2150 cm^{-1} in the low-temperature spectra arises from the diamond ATR cell.

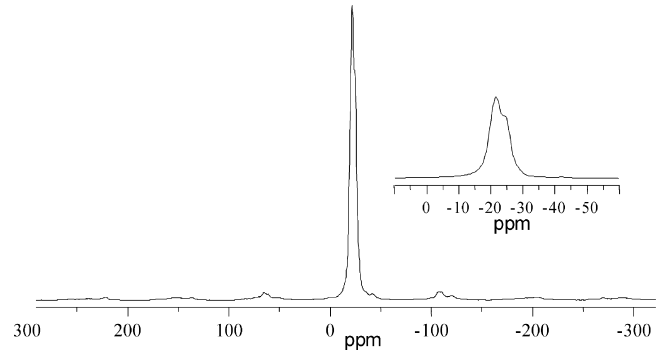

Figure 11. ^{11}B MAS NMR of the ball-milled $2NaBH_4 + ScCl_3$ sample.

Thermal Expansion. The thermal behavior of the $NaSc(BH_4)_4$ lattice parameters is slightly anisotropic, as illustrated in Figures 7 and 8. The volumetric thermal expansion coefficient can be linearly approximated in the interval of 295−408 K (Figure 7) as $\alpha_V = 2.54(3) \times 10^{-4}$ K^{-1}. The *b* lattice parameter shows strong anomaly close to the melting temperature (Figure 8). The thermal behavior of Na_3ScCl_6 lattice parameters in the interval of 295−408 K is given in the Supporting Information in Figures S2 and S3.

Raman and Infrared Spectroscopy. The Raman spectra of sodium and lithium scandium borohydrides, $LiSc(BH_4)_4$ and $NaSc(BH_4)_4$, are compared in Figure 9 and the infrared spectra in Figure 10. It can be seen that the Na and Li compounds present similar Raman spectra over the range from 150 to 2000

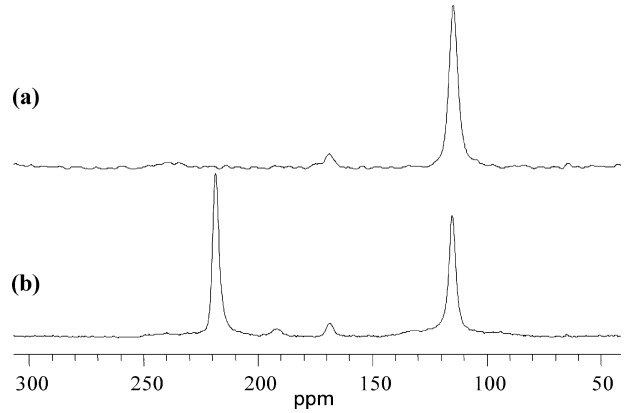

Figure 12. (a) ^{45}Sc [^{1}H] CPMAS-NMR and (b) ^{45}Sc MAS NMR of the ball-milled $2NaBH_4 + ScCl_3$ sample.

cm^{-1}, indicating the presence of a similar $[Sc(BH_4)_4]^-$ anion. However, in the stretching mode region from 2000 to 2600 cm^{-1}, some differences appear: the highest-energy mode, corresponding to the four B−H stretching motions of the outward pointing hydrogen atoms of the $[Sc(BH_4)_4]^-$ anion, is split into two components for the Na compound, while only one component is observed in the spectrum of the Li compound. This is in agreement with the structural difference between Li and Na coordination by hydrogen. In addition, there is a sharp band in the Raman spectrum of the Na-containing sample at 283 cm^{-1}, which corresponds to the totally symmetrical stretching mode of the octahedral $[ScCl_6]^{3-}$ anion in Na_3ScCl_6.[36]

$LiSc(BH_4)_4$ presents in both IR and Raman spectra a band around 1330 cm^{-1} that is not observed in the Raman spectra of the Na compound and appears much weaker in its IR spectrum. Besides this band, the IR spectra of both compounds are rather similar in the BH_4 deformation region between 1000 and 1300 cm^{-1}. The IR spectra measured at approximately 220 K show only a slight sharpening of some bands. Further IR spectra for both samples measured at temperatures down to 170 K did not show additional changes.

NMR Spectroscopy. The magic-angle spinning (MAS) ^{11}B NMR spectrum (see Figure 11) consists of a peak centered at −21.6 ppm that has a prominent upfield shoulder. This indicates that there are two closely related boron chemical environments in $NaSc(BH_4)_4$, which is in accordance with the XRD structure that shows a BH_4 tetrahedron to be present in two different coordination environments. The spectrum also shows that the sample contained a small amount of $NaBH_4$, giving a ^{11}B resonance at 42.2 ppm. The observation of two resonances at 114.7 and 218.6 ppm in the MAS ^{45}Sc NMR spectrum (see Figure 12b) confirms the presence of both $NaSc(BH_4)_4$ and Na_3ScCl_6 in the sample. The former resonance can be assigned to $NaSc(BH_4)_4$ as it alone persists in the ^{1}H CPMAS spectrum (see Figure 12a). The MAS ^{23}Na NMR contains peaks at 0.2, −14.9, and −21.3 ppm. The corresponding CPMAS spectrum again allows assignment of the later resonance to sodium in $NaSc(BH_4)_4$. The remaining two resonances can be assigned to the two differing types of Na in the crystal structure of Na_3ScCl_6. The observed ^{11}B and ^{45}Sc chemical shifts are similar but significantly different from those previously reported for $LiSc(BH_4)_4$ (^{11}B, −23.0 ppm; ^{45}Sc, 113.3 ppm).[37]

Relation to Other Structures. $NaSc(BH_4)_4$ is a new example of a growing family of alkaline or alkaline earth metal and transition-metal homoleptic borohydrides with the general formula, $A^{+m}M^{+n}(BH_4)_{m+n}$, whose crystal structure is described. Several compounds within this class of materials were reported

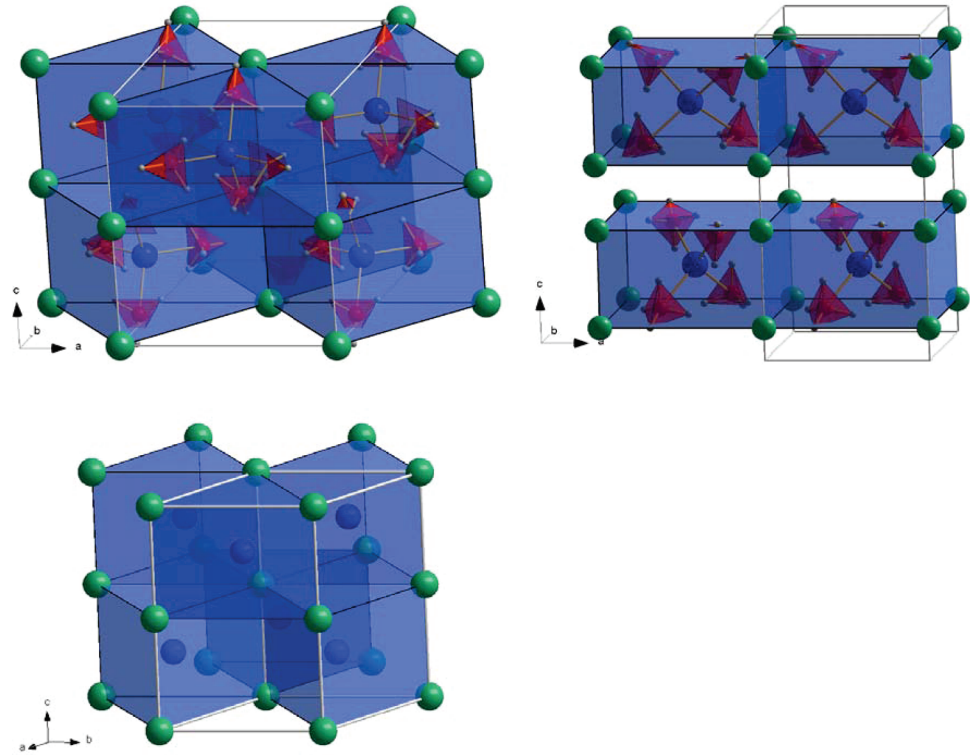

Figure 13. Crystal structure of $NaSc(BH_4)_4$ (top left) and of $LiSc(BH_4)_4$ (top right) viewed approximately along the *b* axes, showing the coordination of Sc atoms (blue) by BH4 tetrahedra (red). The $[Sc(BH_4)_4]$ anions are located inside slightly deformed trigonal prisms Na_6 (each second prism is empty) in $NaSc(BH_4)_4$ (triangular angles of 55.5 and 69.1°) and inside tetragonal prisms Li8 (all prisms occupied) in $LiSc(BH_4)_4$. The Li position is disordered along the *c* axis in $LiSc(BH_4)_4$.[9] The packing of Na^+ cations and $[Sc(BH_4)_4]^-$ anions in $NaSc(BH_4)_4$ corresponds to a distorted variant of the hexagonal NiAs structure type (bottom: Ni, green; As, blue).

in the literature with the tentative compositions $LiZn(BH_4)_3$, $Li_2Zn(BH_4)_4$, $NaZn(BH_4)_3$, $BaZn_3(BH_4)_8$,[38] and $K_2Zn_3(BH_4)_8$,[39,40] and the crystals structures of $LiSc(BH_4)_4$,[9] $LiZn_2(BH_4)_5$, $NaZn_2(BH_4)_5$, $NaZn(BH_4)_3$,[7] and $KZn(BH_4)Cl_2$[8] were recently determined.

In both scandium-based compounds, $LiSc(BH_4)_4$ and $NaSc(BH_4)_4$, the $[Sc(BH_4)_4]^-$ anion is located inside alkaline metal cages (Figure 13): slightly deformed trigonal Na_6 prisms (each second prism is empty) in $NaSc(BH_4)_4$ (triangular angles of 55.5 and 69.1°) and tetragonal Li_8 prisms (all prisms occupied) in $LiSc(BH_4)_4$. Please note that the Li position is disordered along the *c* axis in $LiSc(BH_4)_4$[9] and, therefore, the exact shape of the Li_8 polyhedra remains to be determined.

The packing of Na^+ cations and $[Sc(BH_4)_4]^-$ anions in $NaSc(BH_4)_4$ forms a distorted variant of the hexagonal NiAs structure type (*hP*4; s.g., $P6_3/mmc$) with Na^+ placed on the Ni positions (Figure 13). As the NiAs structure type can be considered as an ordered binary variant of the hcp structure, it shows that the primary building principle in $NaSc(BH_4)_4$ is the close packing of Na^+ cations and $[Sc(BH_4)_4]^-$ anions. It is interesting to note that the true symmetry of the NiAs slightly deviates from the hexagonal and was also found to be orthorhombic ($Cmc2_1$); however, the hexagonal symmetry is simulated in the majority of samples by triple twinning.[41]

Conclusions

$NaSc(BH_4)_4$ is a new example of an alkaline transition-metal borohydride, $A^{+m}M^{+n}(BH_4)_{m+n}$, whose crystal structure is described. A new ternary chloride Na_3ScCl_6, isostructural to Na_3TiCl_6, was identified as a second phase in all samples. This indicates that the formation reaction during ball-milling of $NaBH_4$ and $ScCl_3$ is a complex reaction, which may involve formation of NaCl as an intermediate phase. The new compounds, $NaSc(BH_4)_4$ and Na_3ScCl_6, have been studied by using a combination of in situ synchrotron powder diffraction; thermal analysis; and MAS NMR, Raman, and infrared spectroscopy. The structure of $NaSc(BH_4)_4$ consists of isolated $[Sc(BH_4)_4]^-$ anions located inside slightly deformed trigonal Na_6 prisms, where each second prism is empty. The experimental results show that each Sc^{3+} is tetrahedrally surrounded by four BH_4 tetrahedra with a 12-fold coordination to hydrogen. Compared with $LiSc(BH_4)_4$, the $[Sc(BH_4)_4]^-$ anion in $NaSc(BH_4)_4$ is less deformed. On the other hand, the sodium atoms are surrounded by six BH_4 tetrahedra in a quite regular octahedral coordination with a (6 + 12)-fold coordination to hydrogen.

The packing of Na^+ cations and $[Sc(BH_4)_4]^-$ anions in the structure of $NaSc(BH_4)_4$ forms a distorted variant of the hexagonal NiAs structure type, showing close packing of cations and anions as a primary structural building principle.

Preparation of bimetallic alkaline transition-metal borohydrides allows tuning the desorption properties of borohydrides between stable alkaline metal and unstable transition-metal borohydrides. The sodium scandium borohydride melts at ~410 K and releases the hydrogen in two rapidly occurring steps between 440 and 490 K and 495 and 540 K. This observation is noteworthy in view of the compound's high gravimetric hydrogen content of 12.6 wt %. Furthermore, scandium boride ScB_x may form as a decomposition product, which means that boron is stabilized in the solid dehydrogenated phase; hence, rehydrogenation of the decomposition products might be possible.

Acknowledgment. G.S. and C.M.J. acknowledge the financial support of the Office of Hydrogen Fuel Cells and Infrastructure Technology of the U.S. Department of Energy for their portion of this work. The Danish National Research council under the program DanScatt is thanked for financial support. This work was supported by the Swiss National Science Foundation. The authors acknowledge SNBL for the beamtime allocation.

Supporting Information Available: Tables of atomic positions, representative Rietveld refinement profile, and crystal data. This material is available free of charge via the Internet at http://pubs.acs.org.

References and Notes

(1) Soloveichik, G. *Mater. Matters (Aldrich)* **2007**, *2*, 11–14.
(2) Orimo, S.; Nakamori, Y.; Eliseo, J. R.; Züttel, A.; Jensen, C. M. *Chem. Rev.* **2007**, *107*, 4111–4132.
(3) Grochala, W.; Edwards, P. P. *Chem. Rev.* **2004**, *104*, 1283–1315.
(4) Nakamori, Y.; Miwa, K.; Ninomiya, A.; Li, H.-W.; Ohba, N.; Towata, S.; Züttel, A.; Orimo, S. *Phys. Rev. B* **2006**, *74*, 045126.
(5) Li, H.-W.; Orimo, S.; Nakamori, Y.; Miwa, K.; Ohba, N.; Towata, S.; Züttel, A. *J. Alloys Compd.* **2007**, *446*−*447*, 315–318.
(6) Filinchuk, Y.; Chernyshov, D.; Dmitriev, V. *Z. Kristallogr.* **2008**, *223*, 649–659.
(7) Ravnsbæk, D.; Filinchuk, Y.; Cerenius, Y.; Jakobsen, H. J.; Besenbacher, F.; Skibsted, J.; Jensen, T. R. *Angew. Chem., Int. Ed.* **2009**, *48*, 6659–6663.
(8) Ravnsbæk, D.; Sørensen, L. H.; Filinchuk, Y.; Cerenius, Y.; Jakobsen, H. J.; Besenbacher, F.; Skibsted, J.; Jensen, T. R. *Chem. Commun.* **2009**, submitted.
(9) Hagemann, H.; Longhini, M.; Kaminski, J. W.; Wesolowski, T. A.; Černý, R.; Penin, N.; Sorby, M. H.; Hauback, B. C.; Severa, G.; Jensen, C. M. *J. Phys. Chem. A* **2008**, *112*, 7551–7555.
(10) Kim, Ch.; Hwang, S. J.; Bowman, R. C., Jr.; Reiter, J. W.; Zan, J. A.; Kulleck, J. G.; Kabbour, H.; Majzoub, E. H.; Ozolins, V. *J. Phys. Chem. C* **2009**, *113*, 9956–9968.
(11) Mammen, C. B.; Ursby, T.; Cerenius, Y.; Thunnissen, M.; Als-Nielsen, J.; Larsen, S.; Liljas, A. *Acta Phys. Pol., A* **2002**, *101*, 595–602.
(12) Clausen, B. S.; Steffensen, G.; Fabius, B.; Villadsen, J.; Feidenhans'l, R.; Topsøe, H. *J. Catal.* **1991**, *132*, 524–535.
(13) Ravnsbæk, D.; Mosegaard, L.; Jørgensen, J. E.; Jensen, T. R. *Proceedings of the 29th Risø International Symposium on Materials Science: Energy Materials - Advances in Characterization, Modelling and Application*, Roskilde, Denmark, July 15, 2008.
(14) Hammersley, A. P.; Svensson, S. O.; Hanfland, M.; Fitch, A. N.; Häusermann, D. *High Pressure Res.* **1996**, *14*, 235–248.
(15) Boultif, A.; Louer, D. *J. Appl. Crystallogr.* **2004**, *37*, 724.
(16) Favre-Nicolin, V.; Černý, R. *J. Appl. Crystallogr.* **2002**, *35*, 734.
(17) Coelho, A. A. TOPAS-Academic. http://members.optusnet.com.au/~alancoelho.
(18) Spek, A. L. *PLATON*; University of Utrecht: The Netherlands, 2006.
(19) Efron, B.; Tibshirani, R. *Stat. Science* **1986**, *1*, 54–77.
(20) Hinz, D.; Gloger, T.; Meyer, G. *Z. Anorg. Allg. Chem.* **2000**, *626*, 822–824.
(21) Nakamori, Y.; Li, H.-W.; Kikuchi, K.; Aoki, M.; Miwa, K.; Towata, S.; Orimo, S. *J. Alloys Compd.* **2007**, *446*−*447*, 296–300.
(22) Mosegaard, L.; Møller, B.; Jørgensen, J.-E.; Filinchuk, Y.; Cerenius, Y.; Hanson, J.; Dimasi, E.; Besenbacher, F.; Jensen, T. *J. Phys. Chem. C* **2008**, *112*, 1299–1303.
(23) Arnbjerg, L. M.; Ravnsbæk, D.; Filinchuk, Y.; Vang, R. T.; Cerenius, Y.; Besenbacher, F.; Jørgensen, J.-E.; Jacobsen, H. J.; Jensen, T. R. *Chem. Mater.* **2009**, *2*, 5772−5782.
(24) Filinchuk, Y.; Černý, R.; Hagemann, H. *Chem. Mater.* **2009**, *21*, 925–933.
(25) Filinchuk, Y.; Hagemann, H. *Eur. J. Inorg. Chem.* **2008**, 3127–3133.
(26) Černý, R.; Filinchuk, Y.; Hagemann, H.; Yvon, K. *Angew. Chem., Int. Ed.* **2007**, *46*, 5765–5767.
(27) Soulié, J.-P.; Renaudin, G.; Černý, R.; Yvon, K. *J. Alloys Compd.* **2002**, *346*, 200–205.
(28) Filinchuk, Y.; Chernyshov, D.; Černý, R. *J. Phys. Chem. C* **2008**, *112*, 10579–10584.
(29) Filinchuk, Y.; Chernyshov, D.; Nevidomskyy, A.; Dmitriev, V. *Angew. Chem., Int. Ed.* **2008**, *47*, 529–532.
(30) Nickels, E. A.; Jones, M. O.; David, W. I. F.; Johnson, S. R.; Lowton, R. L.; Sommariva, M.; Edwards, P. P. *Angew. Chem., Int. Ed.* **2008**, *47*, 2817–2819.
(31) Bird, P. H.; Churchill, M. R. *Chem. Commun.* **1967**, 403–405.

(32) (a) Fischer, P.; Züttel, A. *Mater. Sci. Forum* **2004**, *443*−*444*, 287–290. (b) Filinchuk, Y.; Talyzin, A. V.; Chernyshov, D.; Dmitriev, V. *Phys. Rev. B* **2007**, *76*, 092104.

(33) Buchter, F.; £odziana, Z.; Remhof, A.; Friedrichs, O.; Borgschulte, A.; Mauron, Ph.; Züttel, A.; Sheptyakov, D.; Barkhordarian, G.; Bormann, R.; Chłopek, K.; Fichtner, M.; Sørby, M.; Riktor, M.; Hauback, B.; Orimo, S. *J. Phys. Chem. C* **2008**, *112*, 8042–8048.

(34) Filinchuk, Y.; Rönnebro, E.; Chandra, D. *Acta Mater.* **2009**, *57*, 732–738.

(35) Černý, R.; Penin, N.; Hagemann, H.; Filinchuk, Y. *J. Phys. Chem. C* **2009**, *113*, 9003–9007.

(36) Zissi, G. D.; Papatheodorou, G. N. *Chem. Phys. Lett.* **1999**, *308*, 51–57.

(37) Hwang, S.-J.; Bowman, R. C., Jr.; Reiter, J. W.; Rijssenbeek, J.; Soloveichik, G. L.; Zhao, J.-C.; Kabbour, H.; Ahn, C. C. *J. Phys. Chem. C* **2008**, *112*, 3164–3169.

(38) Nöth, H.; Wiberg, E.; Winter, L. P. *Z. Anorg. Allg. Chem.* **1971**, *386*, 73–86.

(39) Hagenmuller, P.; Rault, M. *C. R. Acad. Sci.* **1959**, *248*, 2758–2760.

(40) Mal'tseva, N. N.; Sheiko, O. V.; Bakulina, V. M.; Mikheeva, V. I. *Russ. J. Inorg. Chem.* **1970**, *15*, 363–364.

(41) Thompson, J. G.; Rae, A. D.; Withers, R. L.; Welberry, T. R.; Willis, A. C. *J. Phys. C: Solid State Phys.* **1988**, *21*, 4007–4015.

JP908397W